The pseudophosphatase phogrin enables glucose-stimulated insulin signaling in pancreatic β cells

Received for publication, October 5, 2017, and in revised form, February 14, 2018 Published, Papers in Press, February 26, 2018, DOI 10.1074/jbc.RA117.000301

Seiji Torii[‡1], Chisato Kubota[‡], Naoya Saito[‡], Ayumi Kawano[‡], Ni Hou[‡2], Masaki Kobayashi[§], Ryoko Torii[‡], Masahiro Hosaka[¶], Tadahiro Kitamura[§], Toshiyuki Takeuchi[‡‖], and Hiroshi Gomi[**]

*From the [‡]Biosignal Research Center and [§]Metabolic Signal Research Center, Institute for Molecular and Cellular Regulation, Gunma University, Maebashi, Gunma 371-8512, Japan, the [¶]Department of Biotechnology, Akita Prefectural University, Akita 010-0195, Japan, the [‖]Administration Office, Gunma University, Maebashi, Gunma 371-8512, Japan, and the **Department of Veterinary Anatomy, College of Bioresource Sciences, Nihon University, Fujisawa, Kanagawa 252-8510, Japan*

Edited by Jeffrey E. Pessin

Autocrine insulin signaling is critical for pancreatic β-cell growth and activity and is at least partially controlled by protein-tyrosine phosphatases (PTPs) that act on insulin receptors (IRs). The receptor-type PTP phogrin primarily localizes on insulin secretory granules in pancreatic β cells. We recently reported that phogrin knockdown decreases the protein levels of insulin receptor substrate 2 (IRS2), whereas high-glucose stimulation promotes formation of a phogrin–IR complex that stabilizes IRS2. However, the underlying molecular mechanisms by which phogrin affects IRS2 levels are unclear. Here, we found that relative to wildtype mice, IRS2 levels in phogrin-knockout mice islets decreased by 44%. When phogrin was silenced by shRNA in pancreatic β-cell lines, glucose-induced insulin signaling led to proteasomal degradation of IRS2 via a negative feedback mechanism. Phogrin overexpression in a murine hepatocyte cell line consistently prevented chronic insulin treatment–induced IRS2 degradation. *In vitro*, phogrin directly bound the IR without the assistance of other proteins and protected recombinant PTP1B from oxidation to potentiate its activity toward the IR. Furthermore, phogrin expression suppressed insulin-induced local generation of hydrogen peroxide and subsequent PTP1B oxidation, which allowed progression of IR dephosphorylation. Together, these results suggest that a transient interaction of phogrin with the IR enables glucose-stimulated autocrine insulin signaling through the regulation of PTP1B activity, which is essential for suppressing feedback-mediated IRS2 degradation in pancreatic β cells.

Pancreatic β cells synthesize and secrete the pivotal hormone insulin, which regulates glucose homeostasis and nutrient storage by activating its specific receptor in central and peripheral tissues. β cells express insulin receptor (IR)[3] and its downstream signal pathway components, and genetic studies showed that several elements of this pathway play an essential role in β-cell growth and function (1–3). Mice lacking IR in β cells exhibit decreased levels of glucose-stimulated insulin secretion (GSIS) as well as age-dependent reductions in β-cell mass, whereas insulin receptor substrate 2 (IRS2) knockout mice develop diabetes due to a defect in compensatory β-cell proliferation (4–6). Importantly, expression of insulin signaling proteins is reportedly decreased in islets from patients with type 2 diabetes (7).

Despite the growing evidence of the significance of insulin signaling in β cells, whether secreted insulin acts on its own receptor in an autocrine/paracrine fashion remains controversial (8). Insulin signaling in response to glucose was impaired in β-cell lines derived from IR- or IRS2-knockout mice (9) and in cells of the mouse insulinoma line MIN6 that have siRNA-induced silencing of IR expression (10). Additionally, antibodies specific to insulin could abrogate glucose-stimulated MIN6 proliferation (11), which suggests that secreted insulin has an autocrine or paracrine effect on pancreatic β cells (12, 13). On the other hand, exogenous insulin rather than glucose stimulation reportedly promotes proliferation of primary mouse islet β cells (14), and only low concentrations of insulin could protect primary islet cells from apoptosis (15). However, there is the possibility that β cells could be exposed to high levels of insulin or continuously stimulated by extracellular insulin within the islet. If this is the case, chronic insulin stimulation or high local concentrations of insulin may drive β cells into an insulin-resistant state through desensitization of the insulin-signaling pathway (8).

In the IR- and IRS-signaling pathways, protein-tyrosine phosphatases (PTPs), such as PTP1B and TCPTP, are largely

This work was supported by Grants-in-Aid from the Japanese Society for the Promotion of Science (JSPS KAKENHI, Grant 24390050) and in part by the joint research program of the Institute for Molecular and Cellular Regulation, Gunma University (Grants 12026 and 14022) and in part by the Suzuken Memorial Foundation. The authors declare that they have no conflicts of interest with the contents of this article.

This article contains Figs. S1–S3.

[1] To whom correspondence should be addressed: Biosignal Research Center, Institute for Molecular and Cellular Regulation, Gunma University, Maebashi, Gunma 371-8512, Japan. Tel.: 81-27-220-8859; Fax: 81-27-220-8896; E-mail: storii@gunma-u.ac.jp.

[2] Present address: School of Basic Medical Sciences, Xi'an Jiaotong University Health Science Center, Xi'an, Shaanxi, China.

[3] The abbreviations used are: IR, insulin receptor; EGFP, enhanced green fluorescent protein; GSIS, glucose-stimulated insulin secretion; GST, glutathione *S*-transferase; HG, high glucose; IRS, insulin receptor substrate; KO, knockout; LG, low glucose; PTP, protein-tyrosine phosphatase; ROS, reactive oxygen species; RIP, rat insulin promoter; CPE, carboxypeptidase E; SgIII, secretogranin III; PI3K, phosphatidylinositol 3-kinase; mTOR, mechanistic target of rapamycin; JNK, c-Jun N-terminal kinase; pNPP, *p*-nitrophenyl phosphate; ERK, extracellular signal-regulated kinase; FBS, fetal bovine serum; MEMα, minimum Eagle's medium; CM-H_2DCFDA, 5-(and-6-)chloromethyl-2′,7′-dichlorodihydrofluorescein diacetate; HNMPA(AM_3), hydroxy-2-naphthalenylmethylphosphonic acid trisacetoxymethyl ester.

responsible for returning cells to a basal state by dephosphorylating tyrosine-phosphorylated IRs or IRSs (16, 17). In pancreatic β cells, PTP1B is reportedly involved in dephosphorylating IR (18). Like other tyrosine receptors, IR activation induces reactive oxygen species (ROS) generation, presumably by inactivating cytosolic peroxiredoxins and activating membrane-anchored NADPH oxidases, and the resulting ROS can specifically and transiently inhibit PTP activity by reversible oxidation (19, 20). Because IR phosphotyrosines are dephosphorylated by restored PTPs, PTP oxidation probably plays an important role in determining the duration of insulin signaling. However, prolonged insulin stimulation can overcome PTP regulation and result in serine/threonine phosphorylation of IRSs that is mediated by downstream kinases, including Akt, mTOR, and PKC (21). Consequently, IRSs are ubiquitinated and then degraded by the proteasome, thereby preventing further insulin signaling. The desensitization by this negative regulation seems to reflect an insulin-resistant state. Previous reports demonstrated that chronic exposure (>8 h) to high glucose in pancreatic β cells induces IRS2 degradation by a negative feedback pathway (22, 23), as was shown in adipocytes or hepatocytes.

Recently, we proposed one receptor-like PTP as a regulator of autocrine insulin signaling in pancreatic β cells (24). This protein, phogrin (also known as PTPRN2 or IA-2β), is enriched in insulin granules, where it contributes to glucose-stimulated β-cell growth by stabilizing IRS2 expression. Phogrin translocates to the plasma membrane and interacts with IR when insulin exocytosis is induced by glucose. This phogrin-IR interaction is probably functional, because cell growth retardation and degradation of IRS2 by phogrin knockdown were not observed in IR-deficient cells (24). Mice having a global gene deletion of phogrin exhibit mild glucose intolerance and a slight decrease in islet insulin content (25, 26) but no alterations in β-cell proliferation. On the other hand, the phogrin homolog IA-2 (also known as PTPRN or ICA512) protein also presents a growth-promoting function in both β-cell lines and mouse islets (24, 27). Specific knockdown of IA-2 in MIN6 and INS-1E β-cell lines reduces the cell proliferation rate, whereas IA-2– deficient mice have low β-cell regeneration rates after partial pancreatectomy. Phogrin and IA-2 show the highest sequence similarity in the cytoplasmic PTP domain and lack phosphatase activity for general PTP substrates because of amino acid mutations in the evolutionarily conserved catalytic domain (28). In contrast, the N-terminal pro-domain and the membrane-proximal mature domain called matN (also called the ectodomain) are involved in targeting to secretory granules in endocrine cells (29, 30).

We previously showed that phogrin knockdown decreased IRS2 protein levels and promoted growth retardation in MIN6 cells and cultured mouse islets. We also showed that phogrin formed a complex with activated IR, although whether phogrin affects the tyrosine phosphorylation status of IR is unclear. Here, we extend our studies to explore how phogrin regulates insulin signal transduction for pancreatic β-cell growth. We show that phogrin supports PTP1B activity to achieve an overall regulation of glucose-stimulated insulin signaling in β cells.

Results

IRS2 protein in islets is down-regulated by phogrin deletion

To assess the effect of phogrin deletion on pancreatic β cells, phogrin$^{flox/flox}$ mice (Fig. 1*A*) were crossed with rat insulin promoter (RIP)-cre mice to produce conditional knockout mice that have phogrin expression depletion in β cells. Immunohistochemical analysis with phogrin-specific antibodies showed marked reduction of phogrin expression in the center region of islets from RIP-cre$^{+/-}$_phogrin$^{flox/flox}$ (knockout (KO)) mice relative to islets from control (Cre$^{+/-}$_phogrin$^{+/+}$) mice (Fig. 1*B*). Although pancreatic α cells were likely to be stained by the phogrin antibody, nearly complete depletion of phogrin protein in islets of KO mice was observed by immunoblotting analysis (Fig. 1*C*). In contrast, only a moderate decline in phogrin expression was observed in the hypothalamus. The body weights, blood glucose concentrations, and plasma insulin levels were indistinguishable between male control and KO mice (data not shown).

The morphology of pancreatic islets was unchanged by phogrin knockout as analyzed by hematoxylin-eosin staining (not shown), and the β-cell mass per pancreas was similar between 16-week-old control and KO mice as assessed by immunostaining with insulin antibody (0.503% *versus* 0.493%). Although phogrin may not affect development of islet β cells in mice, the incorporation rate of [^{3}H]thymidine in KO islets was slightly less than that of control islets (Fig. 1*D*). Meanwhile, low glucose stress-induced apoptosis was increased in primary β cells prepared from KO islets compared with those from control islets (Fig. 1*E* and Fig. S1). Importantly, adenovirus-mediated expression of phogrin completely restored apoptosis levels to that of control cells. We next examined expression levels of phogrin-associated proteins in the islets of control and KO mice. IRS2 levels in KO mouse islets were consistently lower than those of control mice at different ages (Fig. 1*F* and Fig. S2). This result suggests that the proliferative activity of pancreatic β cells is decreased by phogrin knockout via down-regulation of IRS2 protein levels. A slight reduction in IA-2 protein expression was similarly observed in phogrin-deficient islets, but there were no significant changes in other insulin granule proteins, such as carboxypeptidase E (CPE), secretogranin III (SgIII), Rab27, and VAMP2 (Fig. 1*F*).

Phogrin functions in IRS2-mediated insulin signaling

Silencing of phogrin in pancreatic β cells reportedly induces ubiquitin proteasome-mediated degradation of the IRS2 protein (24). To elucidate the molecular basis of IRS2 down-regulation, we examined whether phogrin modulates glucose-dependent IRS2 increases at mRNA and protein levels using rat insulinoma INS-1E cells. Consistent with results of previous studies (31), high glucose (HG; 25 mM) promoted a significant increase in both IRS2 mRNA and protein levels in control cells (expressing shVector) (Fig. 2*A*). In contrast, IRS2 protein did not increase in response to HG stimulation in phogrin-silenced cells (shPh3), whereas elevation of mRNA levels was unaffected by phogrin knockdown (Fig. 2*A*). Because chronic exposure (>8 h) of pancreatic β cells to HG induces proteasomal degradation of IRS2 through a negative feedback mechanism (phos-

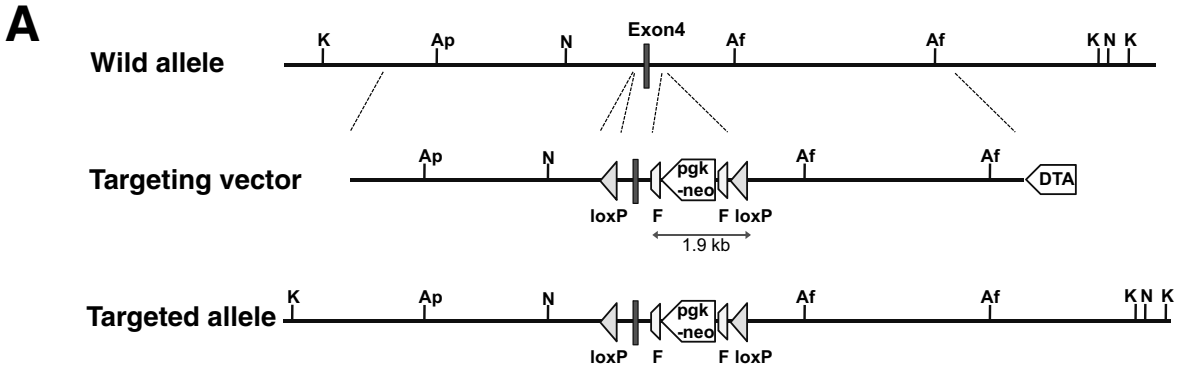
A
Wild allele
K
Ap
N
Exon4
Af
Af
K N K
Targeting vector
Ap
N
pgk
-neo
Af
Af
DTA
loxP
F
F loxP
1.9 kb
Targeted allele
K
Ap
N
pgk
-neo
Af
Af
K N K
loxP
F
F loxP

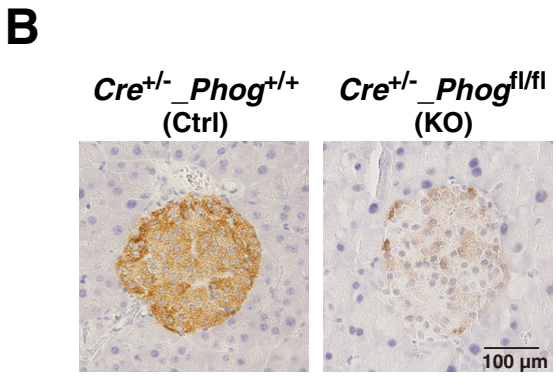
B
Cre+/-_Phog+/+
(Ctrl)
Cre+/-_Phogfl/fl
(KO)
100 µm

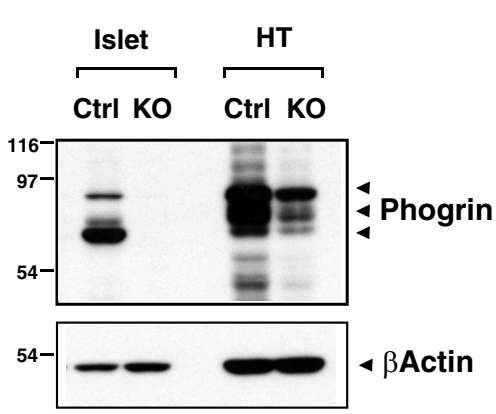
C
Islet
HT
Ctrl KO
Ctrl KO
116
97
54
Phogrin
54
βActin

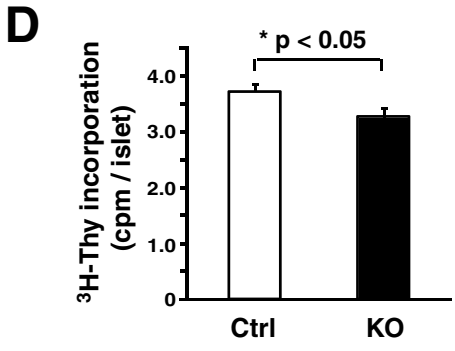
D
* p < 0.05
3H-Thy incorporation
(cpm / islet)
4.0
3.0
2.0
1.0
0
Ctrl
KO

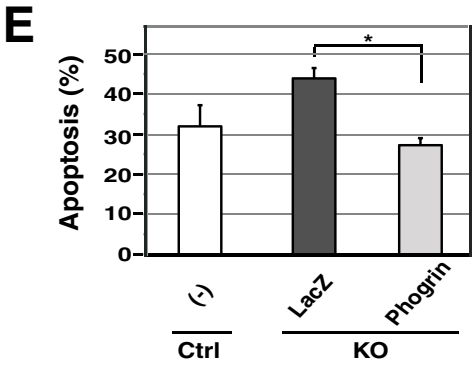
E
Apoptosis (%)
50
40
30
20
10
0
*
(-)
LacZ
Phogrin
Ctrl
KO

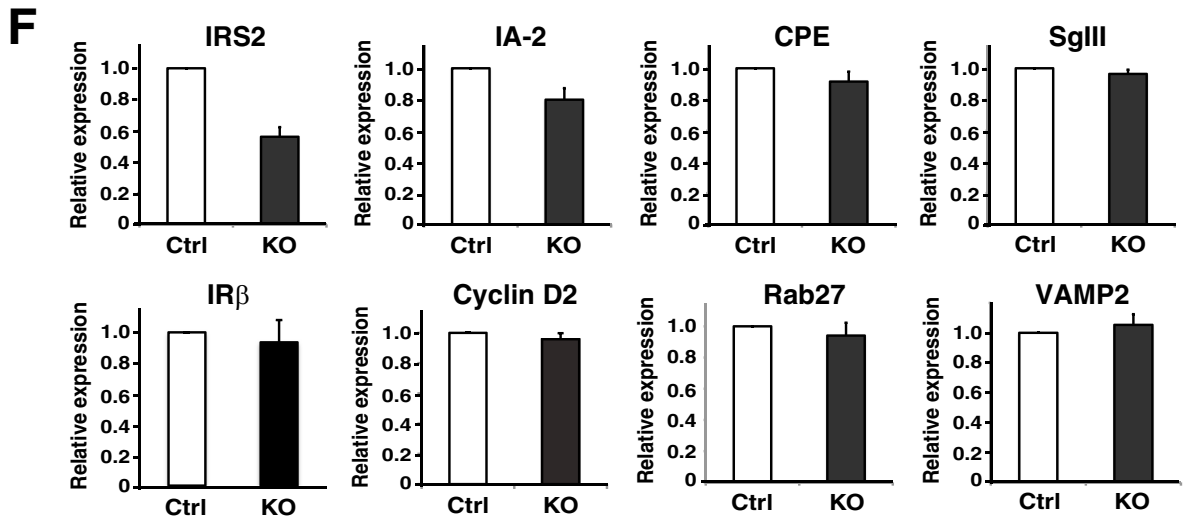
F
IRS2
IA-2
CPE
SgIII
IRβ
Cyclin D2
Rab27
VAMP2
Relative expression
1.0
0.8
0.6
0.4
0.2
0
Ctrl
KO

phatidylinositol 3-kinase (PI3K)-, Akt-, and mTOR-mediated serine phosphorylation of IRS2 and subsequent ubiquitination) (22), we examined whether IRS2 protein levels are reduced by the predicted feedback regulation in the phogrin-knockdown cells. Again, HG culture (4 h)-induced IRS2 protein accumulation was not observed in the shPh3-infected mouse β-cell line MIN6, and in phogrin-silenced cells, IRS2 levels in the HG culture were comparable with that of cells incubated in low glucose (LG; 2 mM) (Fig. 2*B*). IRS2 accumulation in phogrin-silenced cells was completely restored by treatment with the PI3K inhibitors wortmannin and LY294002, the mTOR inhibitor rapamycin, or the c-Jun N-terminal kinase (JNK) inhibitor SP600125 (Fig. 2*B*, *right graph*). Therefore, decreased IRS2 protein in the phogrin-knockdown cells may have resulted from proteasomal degradation via PI3K/mTOR/JNK-mediated signals. Together, these findings suggest that phogrin functions in glucose-regulated insulin-signaling pathways but does not directly stabilize IRS2 protein in pancreatic β cells.

Ubiquitin proteasome-mediated degradation of IRS2 in negative feedback regulation was observed in various insulin-sensitive cells (32). To confirm the involvement of phogrin in insulin signaling, we investigated the effects of phogrin expression in a SV40-transformed mouse hepatocyte cell line (mHEPA). Because non-endocrine cells such as hepatocytes do not express prohormone-processing enzymes and lack hormone-containing secretory granules, for these assays, we used an adenovirus expressing the pro-domain–deleted mature form of phogrin (ΔPro-phogrin). In control cells, prolonged treatment (~8 h) with insulin caused a 45% reduction in levels of the IRS2 protein, whereas chronic insulin treatment did not induce decreases in IRS2 protein in mature phogrin-overexpressing mHEPA cells (Fig. 2*C*). This result demonstrated the potential of phogrin to protect IRS2 from insulin-induced degradation not only in pancreatic beta cells but also in other insulin-sensitive cells.

Phogrin binds to phosphorylated insulin receptor

We previously showed that IRS2 protein expression levels correlated with molecular interactions between phogrin and IR, which are induced by the translocation of phogrin to the plasma membrane of β cells exposed to HG conditions (24). To confirm that transient interactions occur between phogrin and IR in living cells, we used an imaging system based on reconstitution of two split fragments of mKG fluorescent protein (33). Fluorescent signals for mKG were observed only when IR-KGN and phogrin-KGC were cotransfected into MIN6 cells (Fig. S3). We then examined the level of phogrin/IR interaction by a co-immunoprecipitation assay using MIN6 cell lysates. Both the IR kinase inhibitor $HNMPA(AM)_3$ and the PTP inhibitor vanadate blocked the phogrin/IR interaction (data not shown), suggesting that the molecular interaction between IR and phogrin requires both autophosphorylated tyrosine in the IR β subunit and the PTP structure in the phogrin cytoplasmic tail. To determine the phogrin-binding site of IR, three mutants were constructed. In each mutant, the indicated tyrosine(s) was substituted with non-phosphorylatable phenylalanine: Y1F, Tyr-960 of the juxtamembrane domain; Y3F, Tyr-1146, Tyr-1150, and Tyr-1151 in the catalytic domain; Y2F, Tyr-1316 and Tyr-1322 in the C-terminal region. Each IR mutant was EGFP-tagged and expressed in MIN6 cells for coimmunoprecipitation assays. Although the Y2F mutant did not overexpress well (Fig. 3*A*, *left*), the protein content of Y2F and Y3F but not Y1F in the phogrin immunoprecipitates was significantly decreased compared with that of IR-EGFP WT (Fig. 3*A*, *right*). This result suggests that phosphorylated tyrosines in Y2 and Y3 sites are involved in phogrin binding.

Phogrin enhances the ability of PTP1B to dephosphorylate the insulin receptor

Because phogrin and IA-2 both possess an inactive PTP domain in their cytoplasmic regions, we investigated the effects of phogrin on the IR phosphorylation status. We first analyzed whether recombinant phogrin interacts with tyrosine-phosphorylated IR *in vitro*. Cell extracts from insulin-treated COS7 cells expressing IR-EGFP were adsorbed with anti-GFP-agarose. The precipitated IR-EGFP was then incubated with purified glutathione *S*-transferase (GST)-fused PTP proteins, and bound proteins were analyzed by immunoblotting with anti-GST antibody. Both phogrin and IA-2 specifically bound to tyrosine-phosphorylated IR-EGFP, and not to EGFP (data not shown), but this binding was less efficient than TCPTP (Fig. 3*B*). The region within phogrin required for binding to IR was mapped to the cytoplasmic PTP portion (CT). We simultaneously analyzed the tyrosine phosphorylation levels of IR-EGFP with an anti-phosphotyrosine antibody. TCPTP, but neither phogrin nor IA-2, showed dephosphorylation activity against tyrosine-phosphorylated IR-EGFP, although all three proteins were found to interact with this substrate (Fig. 3*C*). We next examined PTP enzyme activity using *p*-nitrophenyl phosphate (pNPP) as a substrate. Again, phogrin and IA-2 showed no phosphatase activity *in vitro* (Fig. 3*D*), which is consistent with previous reports (34). Unexpectedly, however, the mature forms of phogrin and IA-2, but not their truncated versions (matN and CT), enhanced PTP activity of PTP1B by 1.6- and

Figure 1. Reduced IRS-2 expression in phogrin-deficient islets. *A*, schematic diagram of the chromosomal phogrin locus around exon 4 (*bar*) in mice. The targeting vector contains a sequence that includes exon 4 and a neomycin resistance gene driven by the *pgk* promoter (*pgk-neo*), which are both flanked by the *loxP* cassette. Homologous recombination results in replacement of the gene with the targeting sequence. *Ap*, ApaI; *Af*, AflII; *K*, KpnI; *N*, NheI. *B*, pancreatic sections from control (*Ctrl*, $Cre^{+/-}$_$Phogrin^{+/+}$) or KO ($Cre^{+/-}$_$Phogrin^{fl/fl}$) mice were immunostained with anti-phogrin antibodies. *Bar*, 100 μm. *C*, protein extracts were prepared from pancreatic islets and hypothalamus (*HT*) of control (*Ctrl*) and KO mice, and 8 μg of each extract was analyzed by immunoblotting with anti-phogrin or β-actin antibodies. *D*, mouse islets isolated from control or KO mice were incubated with [*methyl*-^{3}H]thymidine, and uptake of [*methyl*-^{3}H]thymidine into islet cell DNA was measured. Data are presented as means ± S.E. (*error bars*) ($n = 4$; *, $p < 0.05$). *E*, islet cells from KO mice were infected separately with adenoviruses integrating β-galactosidase (LacZ) and phogrin at a multiplicity of infection of 10. The infected cells or control islet cells were cultured in RPMI containing 2 mM glucose for 36 h. The apoptosis index of primary β cells was measured by examining nuclear characteristics as described under "Experimental procedures." A representative photograph is shown in Fig. S1. Data are presented as mean ± S.E. ($n = 3$; *, $p < 0.05$). *F*, protein extracts from pancreatic islets of control or KO mice at 16–18 weeks old were analyzed by immunoblotting. Expression levels of IRS2, IA-2, CPE, SgIII, IRβ, cyclin D2, Rab27, or VAMP2 protein quantified by densitometric imaging are shown as -fold increases ± S.E. ($n = 4$) compared with control.

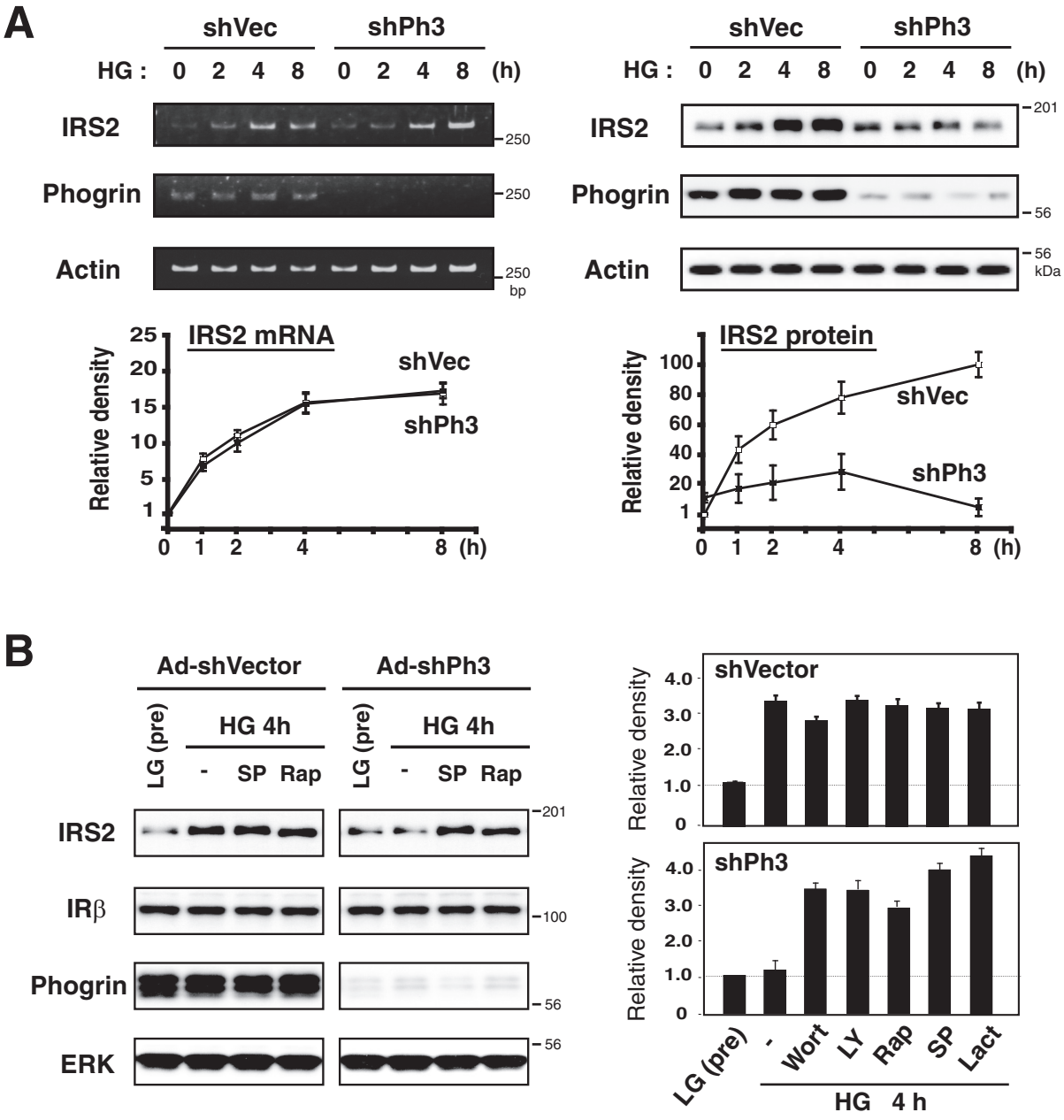
A
shVec
shPh3
HG : 0 2 4 8 0 2 4 8 (h)
IRS2
Phogrin
Actin
250
250
250 bp
201
56
56 kDa
IRS2 mRNA
IRS2 protein
Relative density
shVec
shPh3
0 1 2 4 8 (h)
B
Ad-shVector
Ad-shPh3
LG (pre)
HG 4h
- SP Rap
IRS2
IRβ
Phogrin
ERK
201
100
56
56
shVector
shPh3
Relative density
LG (pre) - Wort LY Rap SP Lact
HG 4 h
C
LacZ
Phogrin (ΔPro)
Insulin 0 5 8 0 5 8 (h)
198
51
99
IRS2
β-Actin
Mature phogrin
Relative expression
0 8 0 8 (h)
LacZ
Phogrin (ΔPro)

1.5-fold, respectively (Fig. 3*D*). An assay using phosphorylated IR-EGFP also showed this enhancing activity of phogrin (Fig. 3*E*), which indicated that phogrin facilitates dephosphorylation of IR only in the presence of PTP1B. In contrast, phogrin did not affect IR tyrosine kinase activity in an *in vitro* IR autophosphorylation assay (data not shown).

The effect of phogrin on IR tyrosine phosphorylation was next explored using β cells and non-β cells. First, we assessed phogrin overexpression using an mHEPA hepatocyte cell line. Insulin treatment of mHEPA cells promptly led to tyrosine phosphorylation of IR, and IR dephosphorylation began after a 10-min incubation in LacZ-expressing control cells (Fig. 4*A*, *left panels*). Exogenous expression of mature phogrin hastened IR dephosphorylation, and the phosphorylation content of IR decreased more rapidly (Fig. 4*A*, *right panels*). Rat insulinoma INS-1E cells were next used to examine autocrine insulin signaling. HG stimulation in INS-1E cells induced tyrosine phosphorylation of IR by 5–10 min, and thereafter, dephosphorylation occurred and returned to basal levels by 20–30 min (Fig. 4*B*). In phogrin-overexpressing cells, the phosphorylation content of IR decreased more rapidly, returning to basal levels within 20 min. Phosphatases do not simply act to terminate a signal but practically contribute to setting the signaling response (35). Thus, our results suggest that phogrin contributes to autocrine insulin signaling by regulating the duration of IR phosphorylation in pancreatic β cells.

Phogrin protects PTP1B from oxidation

Catalytic cysteine residues in PTPs are susceptible to ROS generated upon cell-surface receptor activation, and reversible oxidation of PTPs is involved in downstream signaling (16, 20). We thus examined whether phogrin affects oxidation of recombinant PTP1B. *In vitro*, H_2O_2 treatment (0.1–1 mM) promoted formation of recombinant PTP1B aggregates, which were undetectable by immunoblotting with anti-PTP1B under non-reducing conditions (Fig. 5*A*, *top left*). However, in the presence of reducing agent (2-mercaptoethanol), immunoblotted signals were restored to the control levels (Fig. 5*A*, *top right*). When GST-phogrin was added to the assay, PTP1B oxidation was significantly attenuated even in the presence of 1 mM H_2O_2 (Fig. 5*A*, *left panel* and *graph*). We next investigated intracellular ROS levels by incubating pancreatic β cells with the oxidant probe 5-(and-6-)chloromethyl-2′,7′-dichlorodihydrofluorescein diacetate (CM-H_2DCFDA). Phogrin knockdown in MIN6 cells enhanced intracellular ROS levels, as indicated by green fluorescence of DCF (Fig. 5*B*). Consistently, only weak fluorescence signals were observed in mature phogrin-overexpressing (ΔPro-phogrin) mHEPA hepatocyte cells, although insulin treatment evoked rapid H_2O_2 production in control (LacZ) cells (Fig. 5*C*). These data suggest that phogrin prevents insulin-stimulated H_2O_2 production. We further examined the effect of phogrin expression on insulin-induced oxidation of intracellular PTP1B. Mature phogrin-overexpressing and control mHEPA cells were treated with insulin, and endogenous PTP1B was then immunoprecipitated from the cell lysates. Immunoblotting with anti-Oxi-PTP antibody revealed that phogrin can indeed prevent insulin-induced oxidation of PTP1B in hepatocytes (Fig. 5*D*).

Discussion

Insulin resistance in pancreatic β cells is frequently associated with a decrease in β-cell mass that contributes to type 2 diabetes pathophysiology (3, 36). The finding that chronic stimulation with a high amount of insulin induces proteasomal degradation of IRS2 protein by a negative feedback pathway (22) suggested that insulin released in response to glucose stimulation of β cells does not promote proliferation by the autocrine action of insulin (8). This condition is considered to be an insulin-resistant state in most insulin-sensitive cells. Meanwhile, genetic studies with mice provide evidence that the insulin-signaling pathway plays a critical role in β-cell growth and function (4–6, 37). Furthermore, a compensatory proliferation of β cells in mice is largely dependent on glycolysis and membrane depolarization (38), suggesting that GSIS is coupled to glucose-stimulated β-cell growth. Therefore, if autocrine insulin actions are presumed to occur, β cells might possess specific proteins or mechanisms that suppress the negative feedback pathway of insulin signaling. Because phogrin, an autoantigen of insulin-dependent diabetes mellitus, is highly expressed in pancreatic β cells but not in hepatocytes, adipocytes, and myocytes (28), it may act as a specific regulator of autocrine insulin signaling in pancreatic β cells.

We previously showed that phogrin forms a complex with IR in MIN6 cells when it translocates to the plasma membrane during GSIS activation (24). The interaction of phogrin with IR leads to stabilization of the IRS2 protein that can promote β-cell growth; however, the specific mechanisms of this function are undefined. Here we demonstrate for the first time that phogrin directly binds to IR without the assistance of any other molecules (Fig. 3 and data not shown). Mutation analyses of IR phosphotyrosine residues and co-immunoprecipitation experiments with pharmacological inhibitors suggested that the PTP

Figure 2. Phogrin protects IRS2 protein from proteasomal degradation in both pancreatic β-cell and hepatocyte cell lines. *A*, INS-1E cells were infected with adenoviruses integrating control vector (shVec) or shPhogrin3 (shPh3) for 30 h. After culturing in serum-free RPMI containing 2 mM glucose (LG) and 0.5% BSA for 12 h, cells were stimulated with 16.7 mM glucose (HG) for up to 8 h. Cell extracts and total RNAs were separately prepared. Each RNA sample was analyzed by quantitative RT-PCR analysis with probes for IRS2, phogrin, and actin (*left panels*). Each protein extract was analyzed by immunoblotting with antibodies to IRS2, phogrin, and actin (*right panels*). The intensity of each band was quantified with a densitometer, and the results are presented as -fold increases ± S.E. (*error bars*) compared with time 0 (*bottom graphs*). Experiments were performed three times. *B*, MIN6 cells infected with shVec or shPh3 adenoviruses were stimulated with HG for 4 h with or without 5 μM SP600125 (*SP*) or 50 nM rapamycin (*Rap*). The expression levels of IRS2, IRβ, phogrin, and ERK1/2 were determined by immunoblotting with specific antibodies (*left*). shVec- or shPh3-infected cells were stimulated with HG for 4 h with specific inhibitors: 5 μM SP, 50 nM Rap, 1 μM wortmannin (*Wort*), 50 μM LY294002 (*LY*), or 10 μM lactacystin (*Lact*). Each protein extract was analyzed by immunoblotting with antibodies to IRS2. Band intensity was quantified by densitometry and presented as -fold increase ± S.E. ($n = 3$) compared with unstimulated cells (*right graphs*). *C*, mHEPA hepatocyte cells were infected with LacZ or phogrin adenoviruses that had the pro-region deleted (ΔPro-phogrin). After culturing in serum-free MEMα containing 0.5% BSA for 12 h, cells were stimulated with 100 nM insulin for up to 8 h. The expression levels of IRS2, β-actin, and phogrin were then determined by immunoblotting with specific antibodies (*left*). IRS2 band intensity was quantified by densitometry and presented as -fold increase ± S.E. ($n = 3$) relative to LacZ-expressing control cells (*right*).

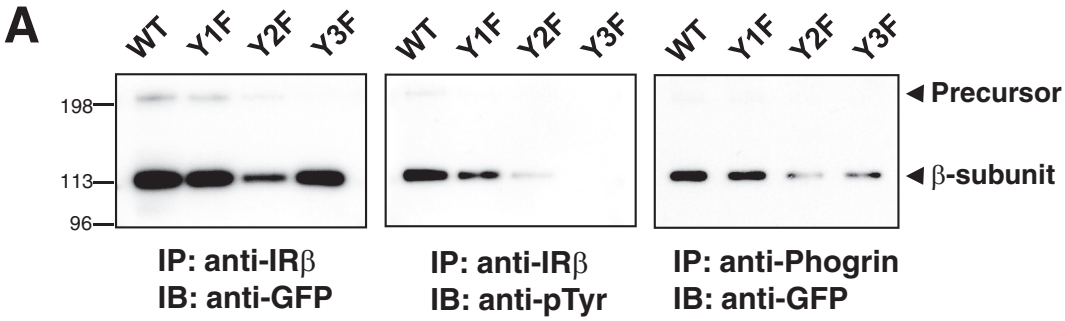
A
WT
Y1F
Y2F
Y3F
198
113
96
Precursor
β-subunit
IP: anti-IRβ
IB: anti-GFP
IP: anti-IRβ
IB: anti-pTyr
IP: anti-Phogrin
IB: anti-GFP

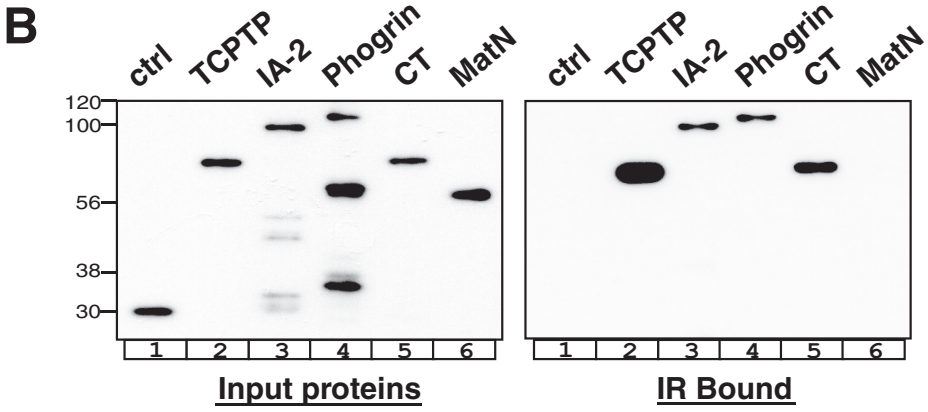
B
ctrl
TCPTP
IA-2
Phogrin
CT
MatN
120
100
56
38
30
1
2
3
4
5
6
Input proteins
IR Bound

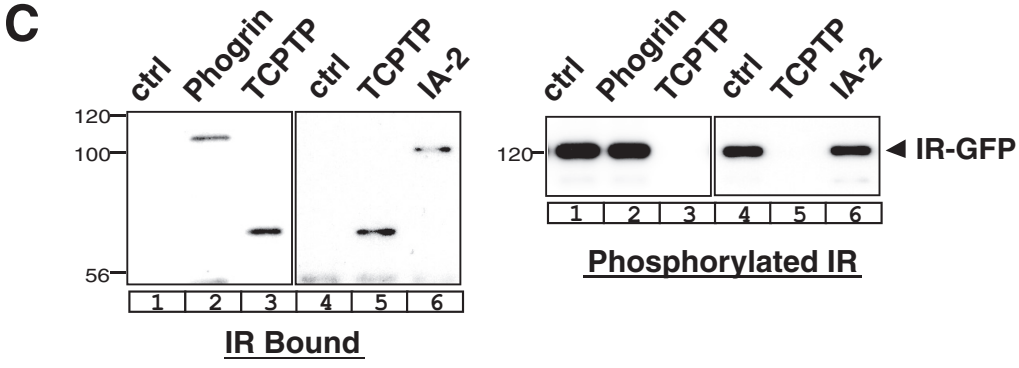
C
ctrl
Phogrin
TCPTP
IA-2
120
100
56
IR-GFP
1
2
3
4
5
6
IR Bound
Phosphorylated IR

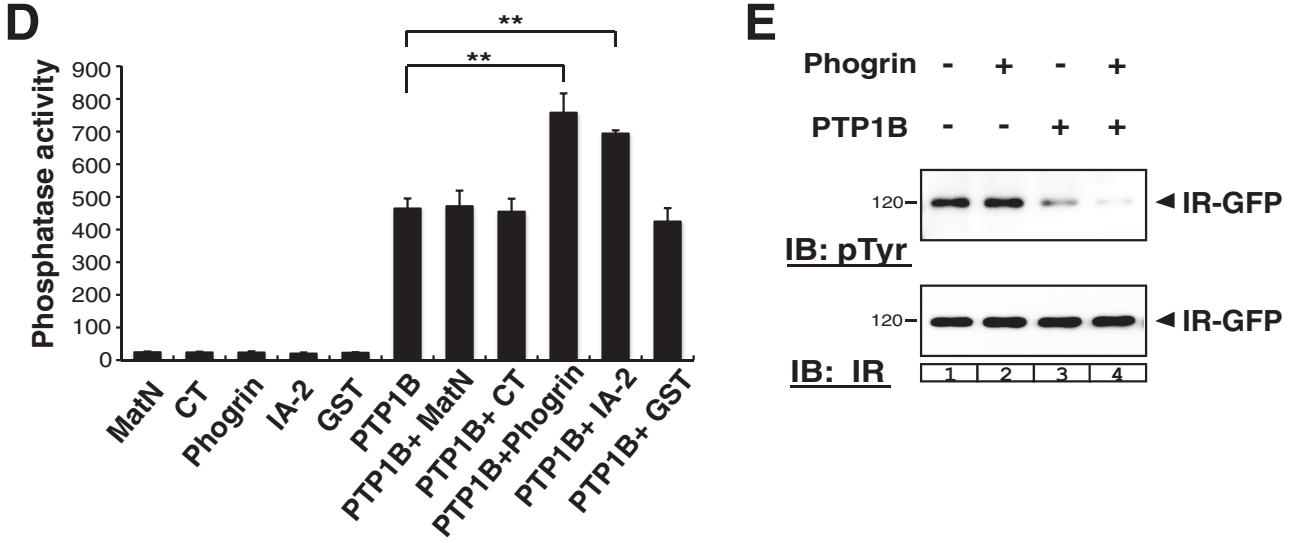
D
Phosphatase activity
900
800
700
600
500
400
300
200
100
0
**
**
MatN
CT
Phogrin
IA-2
GST
PTP1B
PTP1B+ MatN
PTP1B+ CT
PTP1B+Phogrin
PTP1B+ IA-2
PTP1B+ GST
E
Phogrin - + - +
PTP1B - - + +
120
IR-GFP
IB: pTyr
IR-GFP
IB: IR
1
2
3
4

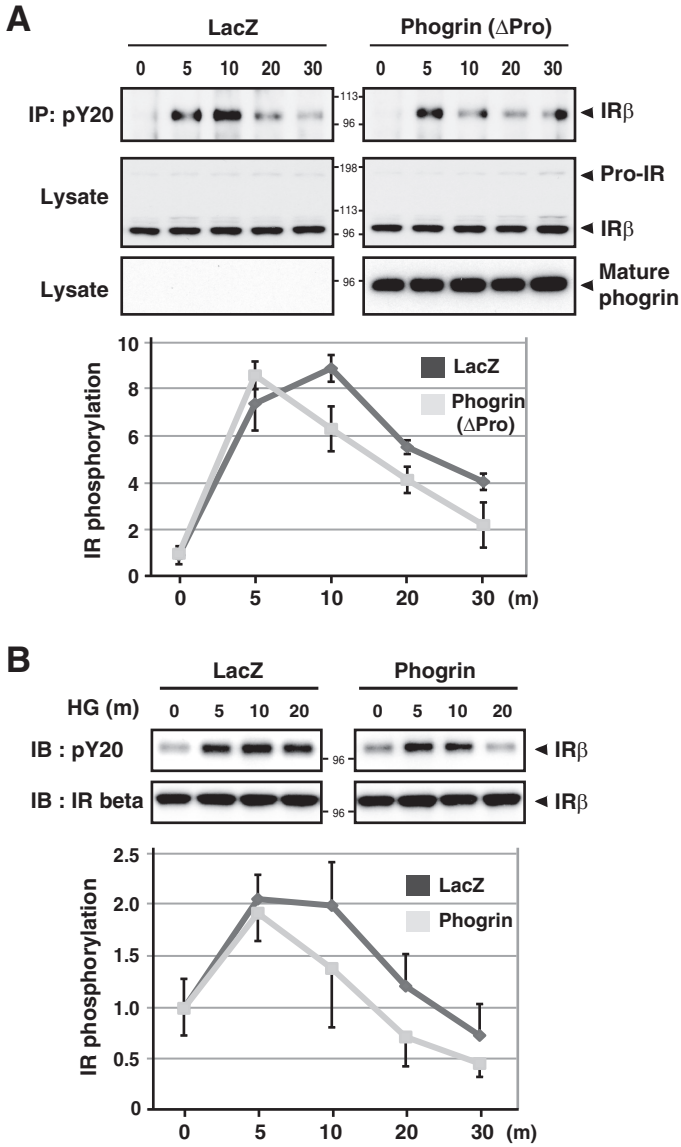

Figure 4. Phogrin accelerates IR dephosphorylation in both hepatocytes and pancreatic β cells. *A*, mHEPA hepatocyte cells were infected with LacZ or ΔPro-phogrin adenoviruses. After culturing in serum-free MEMα containing 0.5% BSA for 12 h, cells were stimulated with 100 nM insulin for the indicated time. Tyrosine phosphorylation state of IR in cell extracts was determined by immunoblotting of anti-phosphotyrosine (pY20) immunoprecipitates (*IP*) with anti-IRβ antibodies. The intensity of each band was quantified by densitometry, and the results are presented as -fold increase ± S.E. (*error bars*) ($n = 3$) relative to the control (time 0) (*bottom graph*). IR and phogrin expression levels were determined by immunoblotting. *B*, INS-1E cells infected by LacZ or phogrin adenoviruses were cultured in serum-free RPMI containing 2 mM glucose and 0.5% BSA for 12 h, preincubated in LG for 2 h, and then stimulated with HG for the indicated time. IR was immunoprecipitated from cell extracts and assessed by immunoblotting with anti-phosphotyrosine antibody (pY20). The same membrane was reprobed with anti-IRβ antibody for a loading control. The intensity of each band (pY20) was quantified by densitometry, and the results are presented as -fold increase ± S.E. ($n = 4$) relative to the control (time 0) (*bottom graph*).

structure of phogrin is primarily involved in its binding to the tyrosine-phosphorylated IR β-subunit (Fig. 3*A* and data not shown). A previous structural study of PTP members demonstrated that the secondary substrate-binding site of the NT1 subgroup represented by PTP1B and TCPTP is distinct from that of the R8 IA-2 family subgroup (39). Indeed, PTP1B targets

Figure 3. Phogrin potentiates PTP1B-mediated IR dephosphorylation. *A*, MIN6 cells transiently transfected with EGFP-tagged wildtype IR (WT) or its point mutants (Y1F, Y2F, and Y3F; see "Experimental procedures") were incubated with HG for 1 h. Expression levels of IR-EGFP were determined by immunoblotting (*IB*) of anti-IR immunoprecipitates (*IP*) with anti-GFP antibodies (*left*). The phosphorylation state of IRβ-EGFP was assessed by immunoblotting of the same immunoprecipitates with anti-phosphotyrosine antibodies (*middle*). Coimmunoprecipitates of anti-phogrin antibodies were analyzed by immunoblotting with anti-GFP antibodies (*right*). *B*, anti-GFP-agarose immunoprecipitates of insulin-treated IR-EGFP were incubated with purified GST (*Ctrl*) or GST-fused TCPTP, IA-2 (mature form; residues 450–979), phogrin (mature form; residues 414–1001), the cytoplasmic region of phogrin (CT; residues 618–1001), or the luminal region of phogrin (MatN; residues 414–599). Bound proteins (*right*) and 10% of the reaction mixture (*left*) were analyzed by immunoblotting with anti-GST monoclonal antibody. *C*, agarose beads containing phosphorylated IR-EGFP were incubated with GST-fused proteins, and interactions were analyzed as in *A* (*left*). The tyrosine phosphorylation levels of IR-EGFP were determined by immunoblotting with anti-phosphotyrosine antibody (*right*). *D*, purified GST or GST-fused phogrin MatN, phogrin CT, phogrin (mature form), or IA-2 with or without recombinant PTP1B were incubated with pNPP as a substrate. Phosphatase activity was determined by measurement of absorbance at 410 nm. Data are presented as mean ± S.E. ($n = 4$; **, $p < 0.05$). *E*, agarose beads carrying phosphorylated IR-EGFP were incubated with purified phogrin and PTP1B (0.8 pmol each). IR-EGFP tyrosine phosphorylation levels were then determined (*top*). Experiments were repeated three times with reproducible results.

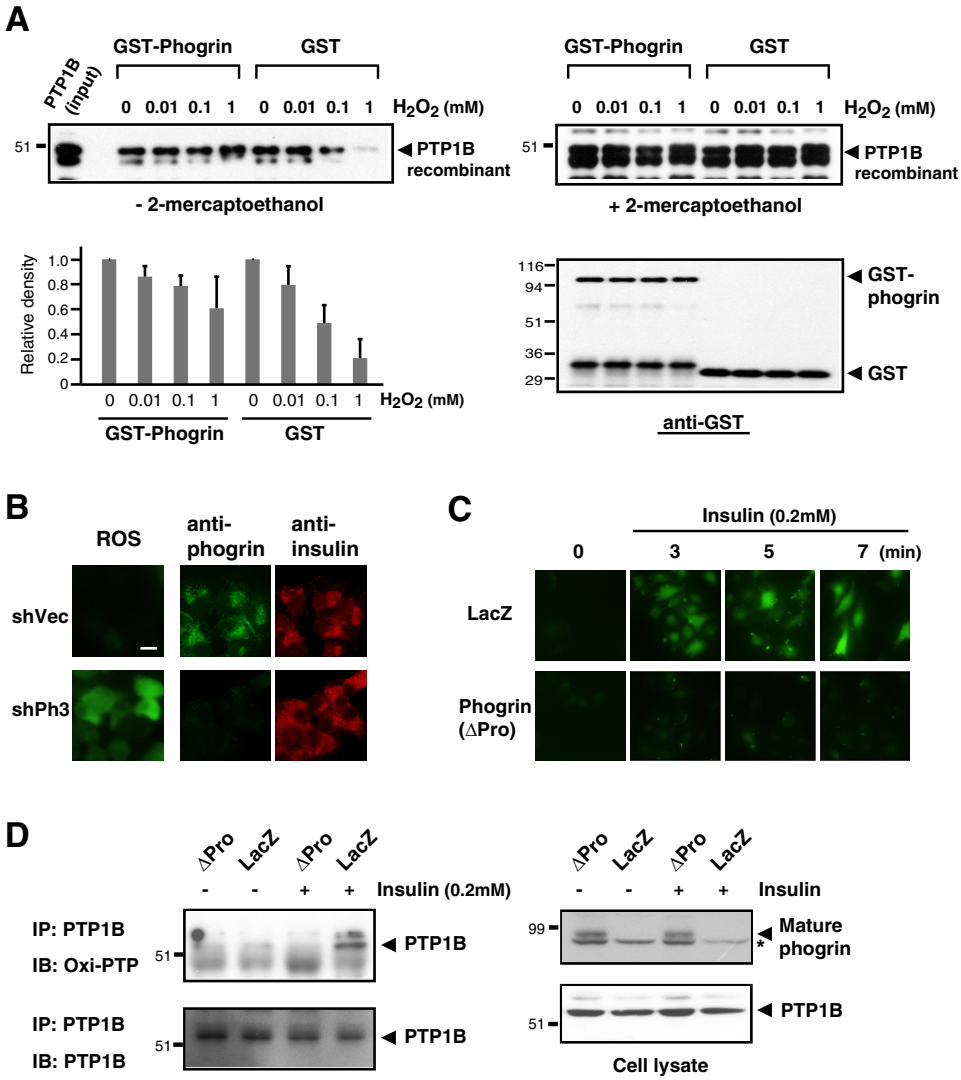

Figure 5. Phogrin protects PTP1B from oxidation. *A*, purified GST or GST-fused phogrin with recombinant PTP1B was treated with increasing amounts of hydrogen peroxide. Equal aliquots of the reaction mixtures were incubated with SDS-PAGE sample buffer with or without 2-mercaptoethanol. The reduced and non-reduced samples were analyzed by immunoblotting with anti-PTP1B monoclonal antibody. Band intensity of non-reduced blotting was quantified by densitometry and presented as -fold increase ± S.E. (*error bars*) ($n = 3$) relative to control (0 mM) (*left graph*). 10% of the reaction mixtures were analyzed by immunoblotting with anti-GST antibody. *B*, MIN6 cells infected with shVec or shPh3 adenoviruses were incubated in the dark with 5 μM CM-H_2DCFDA in Hanks' buffer. DCF fluorescence signals were visualized by microscopy with constant fluorescent parameters (*left panels*). Fixed cells were analyzed by immunostaining with anti-phogrin (*green*) and anti-insulin (*red*) antibodies (*right*). *C*, mHEPA hepatocyte cells infected with LacZ or ΔPro-phogrin adenoviruses were incubated with the probe and stimulated with 200 nM insulin for the indicated time. DCF fluorescence signals were visualized by microscopy with constant fluorescent parameters. Experiments were repeated three times with reproducible results. *D*, mHEPA cells infected with LacZ or ΔPro-phogrin were cultured in serum-free MEMα containing 0.5% BSA for 12 h and stimulated with 200 nM insulin for 5 min. Cell extracts were incubated with anti-PTP1B polyclonal antibodies, and immunoprecipitates (*IP*) were then analyzed by immunoblotting (*IB*) with anti-Oxi-PTP (*top*) or anti-PTP1B (*bottom*) monoclonal antibody. PTP1B and phogrin expression levels were determined by immunoblotting.

the phosphotyrosine in the juxtamembrane Y1 site of IR β-subunit for dephosphorylation (40), whereas mutation of this tyrosine residue did not affect phogrin–IR binding (Fig. 3*A*). This result may explain why phogrin does not compete with PTP1B (TCPTP) for binding to IR (data not shown). Direct interaction of phogrin with IR neither competes with nor inhibits PTP1B-mediated IR dephosphorylation, but phogrin instead potentiates PTP1B phosphatase activity (Fig. 3, *D* and *E*). Notably, the enhancement of PTP1B activity by phogrin required the mature form of phogrin that includes the matN extracellular region, the transmembrane domain, and the cytoplasmic PTP region (CT), whereas the CT fragment alone was sufficient for IR binding (Fig. 3, *B* and *D*). Our coimmunoprecipitation and *in vitro* assays confirmed that phogrin does not directly bind PTP1B (data not shown). These results indicate that molecular interactions of phogrin with IR on the plasma membrane could contribute to spatiotemporal interactions between phogrin and PTP1B in pancreatic β cells. As such, phogrin probably contributes to the enzymatic activity of PTP1B by protecting it from ROS-induced oxidation (Figs. 3 (*D* and *E*) and 5 (*A* and *D*)). However, because we did not identify the oxidative form of phogrin in our assays, the molecular mechanisms by which phogrin performs antioxidant functions require further investigation.

The phogrin-dependent suppression of ROS generation could potentiate PTP1B phosphatase activity, which results in

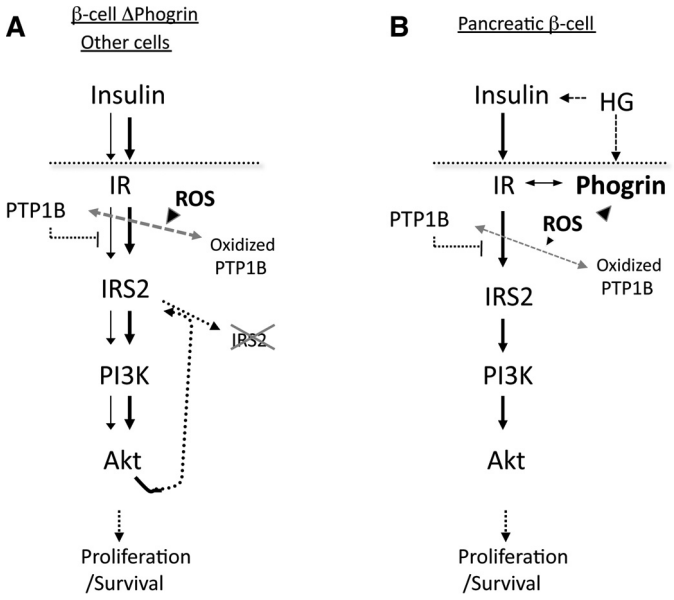

Figure 6. A model for phogrin-mediated regulation of insulin signaling. *A*, in insulin-sensitive cells and β cells with depleted phogrin, insulin activates IR and downstream signaling pathways following transient inactivation of PTP1B by hydrogen peroxide (*thin arrows*). Prolonged activation of IR by insulin induces irreversible oxidation of PTP that can lead to chronic activation of IRS2 signal transduction (*heavy arrows*). After a period of time, internal feedback inhibition signals dampen further activation of IRS2 signaling. In this negative feedback system, Akt and/or TORC1 can phosphorylate IRS2 at serine residues to promote its degradation by the proteasome (*dashed arrows*). *B*, in pancreatic β cells, insulin secretion stimulated by high glucose (GSIS) triggers autocrine- and paracrine-mediated IR activation. GSIS promotes translocation of phogrin to the plasma membrane, where it can interact with activated IR. Localization of phogrin at the IR signaling platform contributes to downstream IRS2 signal transduction by preventing PTP1B oxidation. Dephosphorylation of IR by PTP1B occurs to prevent excess signaling and protects the IRS2 protein from degradation.

prompt IR dephosphorylation (Fig. 4). This transient activation of insulin signaling forms the basis for autocrine insulin action in pancreatic β cells (Fig. 6*B*). When β cells lack phogrin, very high levels of ROS that are probably induced by secreted insulin inactivate PTP1B through irreversible oxidation of the catalytic cysteine. Consequently, autocrine insulin signaling induces a persistent activation of downstream signals (Fig. 6*A*, *heavy line*) that in turn leads to feedback IRS2 down-regulation, as was previously predicted (8). Our earlier data indicated that shRNA-mediated phogrin reduction in β-cell lines or isolated islets led to decreased IRS2 protein levels (24), and here we found that phogrin silencing–induced decreases in IRS2 depend on HG stimulation as well as PI3K-, mTOR-, and JNK-mediated negative feedback mechanisms (Fig. 2*B*). Furthermore, we observed a 44% reduction in IRS2 expression in islets derived from phogrin-knockout mice (Fig. 1*F*). Taken together, our results suggest that phogrin plays an essential role in protecting IRS2 protein from degradation, which allows HG-induced autocrine insulin signaling to proceed (Fig. 6*B*). Meanwhile, when β cells are exposed to LG conditions, phogrin is sequestered in secretory granules, and PTP1B protection does not occur. Therefore, only low concentrations of exogenous insulin promote islet survival in culture, whereas high concentrations of insulin presumably induce oxidative inhibition of PTP1B and the associated feedback down-regulation of IRS2 (15).

In contrast to phogrin, STAT/cyclin-mediated mechanisms are involved in the growth-promoting function of IA-2 (ICA512) (27), suggesting that these two homologous proteins have different functions. Indeed, IA-2 expression in phogrin-deficient islets was slightly decreased rather than increased (Fig. 1*F*). This line of thinking is supported by previous studies showing that β-cell proliferation after partial pancreatectomy is reduced in IA-2– deficient mice (27), whereas IRS2 appears not to have a role in this proliferation (41). Thus, at a mechanistic level, phogrin and IA-2 differ, although their overall regulatory effects on β-cell growth are similar.

Mice that are specifically deficient in IRS2 in β cells and the hypothalamus exhibit an age-dependent reduction in the β-cell mass (42, 43), whereas IRS2 is crucially involved in β-cell proliferation in response to high-fat diet–induced insulin resistance (44). A possible explanation of the unchanged β-cell mass in phogrin-knockout mice is that phogrin regulates β-cell growth only as a compensatory response. Our preliminary experiments show that phogrin-deficient mice fed the high-fat diet had significantly lower compensatory β-cell hyperplasia than did control mice.[4] We presume that phogrin stabilizes the IRS2 protein through interactions with the IR only in response to demands of β-cell mass expansion. Thus, additional studies are needed to elucidate the role of phogrin in β-cell growth.

The present data support our hypothesis that phogrin is a unique regulator of the autocrine insulin signal pathway in pancreatic β cells. Moreover, our data support the existence of a direct autocrine action of insulin, although several questions remain, including what is the behavior of secreted insulin around β cells. We found that microlocalization of phogrin-EGFP at the cell surface overlapped with the punctate signals produced by staining with an anti-IRα subunit antibody (data not shown). Further investigation using recently developed super-resolution microscopy techniques could help visualize extracellular insulin behavior in greater detail, which would provide a further characterization of IR activation microdomains and exocytotic domains of insulin granules.

Experimental procedures

Antibodies and reagents

The anti-phogrin and IA-2 rabbit polyclonal antibodies against the luminal region were affinity-purified (24). These antibodies were previously characterized (24, 45). The guinea pig anti-insulin antibody, anti-β-actin, and anti-GST mouse monoclonal antibodies were purchased from Sigma. Anti-phosphotyrosine mouse (pY20), anti-CPE, and anti-pan-ERK mouse monoclonal antibodies and anti-IRβ rabbit polyclonal antibodies were purchased from BD Biosciences (Lexington, KY). Anti-oxidized PTP active site (Oxi-PTP) mouse monoclonal antibody and anti-PTP1B rabbit polyclonal antibodies were from R&D Systems (Minneapolis, MN). Anti-IRS2 rabbit, anti-Rab27 rabbit, and anti-GFP mouse monoclonal antibodies were from Upstate Biotechnology, Inc. (Lake Placid, NY), Immuno-

[4] S. Torii, C. Kubota, M. Kobayashi, R. Torii, M. Hosaka, T. Kitamura, T. Takeuchi, and H. Gomi, unpublished data.

Biological Laboratories (Gunma, Japan), and Roche Diagnostics, respectively. Anti-PTP1B mouse monoclonal antibody (clone FG6) and SP600125 were purchased from Calbiochem. LY294002 was from Cayman Chemical, and wortmannin, rapamycin, and anti-VAMP2 rabbit antibody were from Wako Chemical (Osaka, Japan). Anti-mKGC mouse monoclonal antibody was from MBL (Nagoya, Japan).

Plasmids

Full-length mouse insulin receptor (type A) was amplified by PCR using a MIN6 library as a template and was cloned into the pcDNA3-EGFP vector (29). Point mutants of three phosphotyrosine sites were generated by PCR using primers Y1F (5′-CGGATGGGCCAATGGGACCACTGTATGCATCTTCAAACCCTGAGTTCCTCAG-3′), Y2F (5′-CCATTCATGTGGGTAAAGGGGATGTGTTCATCAAAGGTCCGTTTG-3′), and Y3F (5′-TTGGAATGACAAGGGACATCTTCGAGACAGATTTCTTTCGGAAAGGGGGC-3′). Truncated fragments of mouse phogrin (residues 414–1001, lacking the signal sequence and pro-region) were constructed by PCR using pcDNA3-phogrin-EGFP as a template and were cloned into the pGEX4T-1 vector (for GST fusion protein) as described previously (29). A fragment of the signal sequence region (residues 1–28) was ligated to construct ΔPro in the adenovirus expression vector pAxCAwt (TaKaRa Biomedicals). Recombinant adenovirus expressing β-galactosidase (LacZ) and shRNA for phogrin (shPh3) were previously characterized (24). The virus titer was expressed as the multiplicity of infection.

Knockout mice

Construction of the targeting vector, homologous recombination using embryonic stem cells (RENKA), and generation of chimeric mice were achieved by Transgenic Inc. (Kobe, Japan). The targeting vector contains a sequence that includes exon 4 of the phogrin gene and a neomycin resistance gene driven by the *pgk* promoter (*pgk-neo*), which are both flanked by the *loxP* cassette. Homologous recombination replaces the gene with the targeting sequence. Mutant lines were maintained by crossing male and female homozygotes. RIP-cre mice (37) were maintained as heterozygotes by backcrossing with C57Bl/6J mice (Japan SLC). Control ($Cre^{+/-}$_$Phogrin^{+/+}$) and knockout ($Cre^{+/-}$_$Phogrin^{flox/flox}$) mice for the experiments were obtained by crossing heterozygotes. Male mice with similar body weights and ages were used for all experiments. Genotype analysis was done by PCR. The primers for Cre were 5′-ACCTGATGGACATGTTCAGGGATCG-3′ and 5′-TCCGGTTATTCAACTTGCACCATGC-3′, and the primers for phogrin and floxed allele were 5′-CCAGCGTGTGATTGCCCAGGAG-3′, 5′-ATTCGCAGCGCATCGCCTTCTATCGCCTTC-3′, and 5′-CCTGCTCATTGCAATGTTGTTAAC-3′. Mice had free access to water and standard laboratory chow (CE-2; CLEA Japan) in an air-conditioned room with a 12-h light/dark cycle. All animal experiments were approved by the Gunma University Animal Care and Experimentation Committee (permission no. 16-017) and were conducted according to its guidelines.

Cell culture and transfection

MIN6 cells before passage 25 were cultured in Dulbecco's modified Eagle's medium with 15% fetal bovine serum (FBS) and 50 μM 2-mercaptoethanol. INS-1E cells were cultured in RPMI1640 with 10% FBS, 10 mM HEPES (pH 7.4), and 50 μM 2-mercaptoethanol. Cells of the murine hepatocyte line were transformed by SV40 large T antigen and cultured in MEMα with 4% FBS (46). Transfections were performed with Lipofectamine 2000 reagent (Invitrogen).

Immunohistochemistry

Immunohistochemical analyses were performed as described previously (45). Paraffin-embedded pancreas sections were labeled with anti-phogrin antibody (1:1,500 dilution) and detected using an avidin-biotin-peroxidase technique (Vector Laboratories) with hematoxylin counterstaining. Image acquisition was completed using a microscope (Olympus BX-50) equipped with a SenSys™ charge-coupled device camera (Photometrics).

Thymidine incorporation and apoptosis analysis

Mouse pancreatic islets were isolated and cultured as described previously (24). After culturing for 48 h, [^{3}H]thymidine was added at a final concentration of 1 mCi/ml to pools of 50 islets for an additional 24 h. The DNA was precipitated with ice-cold 10% trichloroacetic acid and solubilized in 0.3 N NaOH. Aliquots were counted in scintillation fluid, and thymidine incorporation into islet cell DNA was determined. Isolated islets were dispersed into cells with 0.05% trypsin, 0.02% EDTA and cultured on 8-well Lab-Tek chamber slides (Thermo Scientific Nunc) precoated with poly-L-lysine (Sigma). Apoptosis analysis of primary β cells was performed as described previously (47). Briefly, islet cells were fixed with 4% paraformaldehyde and then incubated with anti-insulin followed by Rhodamine Red™-X–conjugated, anti-guinea pig IgG secondary antibody (Jackson ImmunoResearch) to detect β cells. Condensation or fragmentation of nuclei (apoptotic characteristics) was assessed by 4′,6-diamidino-2-phenylindole staining. Insulin-positive islet β cells having normal or apoptotic nuclei were counted, and the cell death rate was calculated. At least 10 different fields from each mouse sample were randomly selected to count at least 100 β cells for calculation of apoptosis rates.

Immunoblot analysis of protein expression

For extraction of total protein, cells were lysed in ice-cold lysis buffer A (20 mM Tris, pH 7.5, 150 mM NaCl, 1% Nonidet P-40, 1 mM EGTA, 10 mM NaF, 10 mM β-glycerophosphate, 0.5 mM sodium orthovanadate, 0.5 mM phenylmethylsulfonyl fluoride, 10 μg/ml aprotinin, 10 μg/ml leupeptin, and 5 μg/ml pepstatin A). Protein samples (8–20 μg) were quickly mixed with electrophoresis sample buffer and stored at −80 °C. Immunoblotting analysis was performed as described previously (48). The blotted membranes were blocked with 5% skim milk and incubated with primary antibodies (1:5,000 dilution for insulin; 1:5,000 for β-actin; 1:4,000 for GST; 1:1,000 for phosphotyrosine; 1:1,500 for CPE; 1:6,000 for ERK; 1:2,000 for IR; 1:1,200

for oxidized PTP; 1:4,000 for IRS2; 1:2,000 for Rab27; 1:1,000 for GFP; 1:800 for PTP1B; 1:5,000 for VAMP2). Band density was measured by densitometry, quantified using gel-plotting macros of the NIH Image version 1.62 program, and normalized to an indicated sample in the same membrane.

Semiquantitative RT-PCR

RT-PCR analysis was performed as described previously (24). Amplified signals stained with ethidium bromide were quantified with an ATTO Cool Saver system (ATTO, Tokyo, Japan).

In vitro assay with GST proteins

An *in vitro* binding assay (29) and dephosphorylation assay (49) were combined. PTP1B and TCPTP cDNAs were subcloned into the pGEX6P-1 vector. Bacterially expressed GST-fused proteins were then affinity-purified with glutathione-Sepharose beads and eluted with reduced glutathione or incubated with PreScission protease (GE Healthcare). Purified proteins were dialyzed with 10 mM Tris buffer. COS7 cells expressing IR-EGFP were treated with 100 nM insulin for 10 min and then extracted with lysis buffer A. IR-EGFP was immunoprecipitated with agarose-conjugated anti-GFP (RQ2, MBL Co.) and washed with PTP buffer (20 mM Tris, pH 6.8, 150 mM NaCl, 2 mM EDTA, 25 mg/ml BSA, and 1 mM dithiothreitol) containing 0.05% Nonidet P-40. IR-EGFP immobilized on agarose beads were incubated at 25 °C with 2 pmol of each GST protein and 1 pmol of recombinant PTP1B in 0.2 ml of PTP buffer for 20 min. The beads were washed three times, and the bound proteins were analyzed by immunoblotting. Each purified GST protein (4 pmol) was preincubated with or without recombinant PTP1B for 10 min. PTP activity was then measured with pNPP as a substrate in a buffer containing 20 mM MES, pH 6.0, 2 mM EDTA, and 10 mM pNPP. The reaction was terminated with NaOH, and absorbance was measured at 410 nm.

Immunoprecipitation analysis

MIN6 cells were extracted with lysis buffer B (20 mM Tris, pH 7.5, 150 mM NaCl, 0.5% Nonidet P-40, 1 mM EGTA, 0.5 mM phenylmethylsulfonyl fluoride, 5 μg/ml aprotinin, 5 μg/ml leupeptin, and 1 μg/ml pepstatin). Cell extracts were incubated with anti-phogrin antibodies (0.5 mg/ml), and the antibodies were collected by agitation with protein G–Sepharose 4FF (GE Healthcare). Immunoprecipitates were subjected to immunoblotting with anti-IR mouse antibody (1:1,000; Merck-Millipore). For analysis of oxidized PTP1B, mouse hepatocytes were extracted with degassed lysis buffer C (25 mM Hepes, pH 7.5, 150 mM NaCl, 1% Nonidet P-40, 10 mM NaF, 10 mM β-glycerophosphate, 5% glycerol, 0.1 units/ml catalase (Calbiochem), 0.1 units/ml superoxide dismutase (Calbiochem), and 10 mM iodoacetamide). Cell extracts were incubated with anti-PTP1B rabbit polyclonal antibodies (5 μl for 0.5 mg of cell extracts), and immunoprecipitates were then analyzed by immunoblotting with anti-Oxi-PTP antibody.

Fluorescence microscopy

MIN6 and hepatocytes were incubated in the dark at 37 °C for 5 min with 5 μM CM-H_2DCFDA (Invitrogen) on poly-L-lysine (Sigma)-coated coverslips. The cells were mounted on a glass slide with Hanks' buffer. DCF fluorescence was observed with an epifluorescence microscope (BX-50) as described previously (50). To avoid photooxidation of the indicator dye, the fluorescence images were collected by a single rapid scan with identical parameters (*e.g.* contrast and brightness) for all samples.

Statistical analysis

Results are given as the mean ± S.E., except when otherwise indicated. Differences between groups were analyzed using Student's t test or the Mann–Whitney U test. p values < 0.05 were considered statistically significant.

Author contributions—S. T. and H. G. conceptualization; S. T. and C. K. data curation; S. T. formal analysis; S. T. funding acquisition; S. T., C. K., N. S., A. K., N. H., and R. T. investigation; S. T., C. K., N. S., A. K., N. H., M. K., M. H., and H. G. methodology; S. T. writing-original draft; S. T. project administration; M. K. and T. K. resources; M. H., T. K., T. T., and H. G. supervision; M. H. validation; T. T. and H. G. writing-review and editing.

Acknowledgments—We thank Drs. N. Aoki (Mie University) and H. Miyazaki (Tsukuba University) for TCPTP and PTP1B plasmids and Drs. K. Aoyagi (Kyorin University), Y. Murata (Kobe University), and S. Mizutani (Gunma University) for technical support. We also thank E. Tajima, M. Kosaki, and M. Hosoi for generous support.

Note added in proof—In the version of this article that was published as a Paper in Press on February 26, 2018, the graph in Fig. 4*A* was missing the "LacZ" label. This error has now been corrected.

References

1. Taniguchi, C. M., Emanuelli, B., and Kahn, C. R. (2006) Critical nodes in signalling pathways: insights into insulin action. *Nat. Rev. Mol. Cell Biol.* **7,** 85–96 CrossRef Medline
2. Leibiger, I. B., Leibiger, B., and Berggren, P. O. (2008) Insulin signaling in the pancreatic beta-cell. *Annu. Rev. Nutr.* **28,** 233–251 CrossRef Medline
3. Goldfine, A. B., and Kulkarni, R. N. (2012) Modulation of beta-cell function: a translational journey from the bench to the bedside. *Diabetes Obes. Metab.* **14,** 152–160 CrossRef Medline
4. Withers, D. J., Gutierrez, J. S., Towery, H., Burks, D. J., Ren, J. M., Previs, S., Zhang, Y., Bernal, D., Pons, S., Shulman, G. I., Bonner-Weir, S., and White, M. F. (1998) Disruption of IRS-2 causes type 2 diabetes in mice. *Nature* **391,** 900–904 CrossRef Medline
5. Kulkarni, R. N., Brüning, J. C., Winnay, J. N., Postic, C., Magnuson, M. A., and Kahn, C. R. (1999) Tissue-specific knockout of the insulin receptor in pancreatic beta cells creates an insulin secretory defect similar to that in type 2 diabetes. *Cell* **96,** 329–339 CrossRef Medline
6. Kubota, N., Tobe, K., Terauchi, Y., Eto, K., Yamauchi, T., Suzuki, R., Tsubamoto, Y., Komeda, K., Nakano, R., Miki, H., Satoh, S., Sekihara, H., Sciacchitano, S., Lesniak, M., Aizawa, S., *et al.* (2000) Disruption of insulin receptor substrate 2 causes type 2 diabetes because of liver insulin resistance and lack of compensatory beta-cell hyperplasia. *Diabetes* **49,** 1880–1889 CrossRef Medline
7. Gunton, J. E., Kulkarni, R. N., Yim, S., Okada, T., Hawthorne, W. J., Tseng, Y. H., Roberson, R. S., Ricordi, C., O'Connell, P. J., Gonzalez, F. J., and Kahn, C. R. (2005) Loss of ARNT/HIF1β mediates altered gene expression and pancreatic-islet dysfunction in human type 2 diabetes. *Cell* **122,** 337–349 CrossRef Medline
8. Rhodes, C. J., White, M. F., Leahy, J. L., and Kahn, S. E. (2013) Direct autocrine action of insulin on beta-cells: does it make physiological sense? *Diabetes* **62,** 2157–2163 CrossRef Medline

9. Assmann, A., Ueki, K., Winnay, J. N., Kadowaki, T., and Kulkarni, R. N. (2009) Glucose effects on beta-cell growth and survival require activation of insulin receptors and insulin receptor substrate 2. *Mol. Cell. Biol.* **29,** 3219–3228 CrossRef Medline
10. Ohsugi, M., Cras-Méneur, C., Zhou, Y., Bernal-Mizrachi, E., Johnson, J. D., Luciani, D. S., Polonsky, K. S., and Permutt, M. A. (2005) Reduced expression of the insulin receptor in mouse insulinoma (MIN6) cells reveals multiple roles of insulin signaling in gene expression, proliferation, insulin content, and secretion. *J. Biol. Chem.* **280,** 4992–5003 CrossRef Medline
11. Muller, D., Jones, P. M., and Persaud, S. J. (2006) Autocrine anti-apoptotic and proliferative effects of insulin in pancreatic beta-cells. *FEBS Lett.* **580,** 6977–6980 CrossRef Medline
12. Martinez, S. C., Cras-Méneur, C., Bernal-Mizrachi, E., and Permutt, M. A. (2006) Glucose regulates Foxo1 through insulin receptor signaling in the pancreatic islet beta-cell. *Diabetes* **55,** 1581–1591 CrossRef Medline
13. Aikin, R., Hanley, S., Maysinger, D., Lipsett, M., Castellarin, M., Paraskevas, S., and Rosenberg, L. (2006) Autocrine insulin action activates Akt and increases survival of isolated human islets. *Diabetologia* **49,** 2900–2909 CrossRef Medline
14. Beith, J. L., Alejandro, E. U., and Johnson, J. D. (2008) Insulin stimulates primary beta-cell proliferation via Raf-1 kinase. *Endocrinology* **149,** 2251–2260 CrossRef Medline
15. Johnson, J. D., Bernal-Mizrachi, E., Alejandro, E. U., Han, Z., Kalynyak, T. B., Li, H., Beith, J. L., Gross, J., Warnock, G. L., Townsend, R. R., Permutt, M. A., and Polonsky, K. S. (2006) Insulin protects islets from apoptosis via Pdx1 and specific changes in the human islet proteome. *Proc. Natl. Acad. Sci. U.S.A.* **103,** 19575–19580 CrossRef Medline
16. Ostman, A., Frijhoff, J., Sandin, A., and Böhmer, F. D. (2011) Regulation of protein tyrosine phosphatases by reversible oxidation. *J. Biochem.* **150,** 345–356 CrossRef Medline
17. Tiganis, T. (2013) PTP1B and TCPTP–nonredundant phosphatases in insulin signaling and glucose homeostasis. *FEBS J.* **280,** 445–458 CrossRef Medline
18. Kushner, J. A., Haj, F. G., Klaman, L. D., Dow, M. A., Kahn, B. B., Neel, B. G., and White, M. F. (2004) Islet-sparing effects of protein tyrosine phosphatase-1b deficiency delays onset of diabetes in IRS2 knockout mice. *Diabetes* **53,** 61–66 CrossRef Medline
19. Meng, T. C., Buckley, D. A., Galic, S., Tiganis, T., and Tonks, N. K. (2004) Regulation of insulin signaling through reversible oxidation of the protein-tyrosine phosphatases TC45 and PTP1B. *J. Biol. Chem.* **279,** 37716–37725 CrossRef Medline
20. Goldstein, B. J., Mahadev, K., Kalyankar, M., and Wu, X. (2005) Redox paradox: insulin action is facilitated by insulin-stimulated reactive oxygen species with multiple potential signaling targets. *Diabetes* **54,** 311–321 CrossRef Medline
21. Copps, K. D., and White, M. F. (2012) Regulation of insulin sensitivity by serine/threonine phosphorylation of insulin receptor substrate proteins IRS1 and IRS2. *Diabetologia* **55,** 2565–2582 CrossRef Medline
22. Briaud, I., Dickson, L. M., Lingohr, M. K., McCuaig, J. F., Lawrence, J. C., and Rhodes, C. J. (2005) Insulin receptor substrate-2 proteasomal degradation mediated by a mammalian target of rapamycin (mTOR)-induced negative feedback down-regulates protein kinase B-mediated signaling pathway in beta-cells. *J. Biol. Chem.* **280,** 2282–2293 CrossRef Medline
23. Gurevitch, D., Boura-Halfon, S., Isaac, R., Shahaf, G., Alberstein, M., Ronen, D., Lewis, E. C., and Zick, Y. (2010) Elimination of negative feedback control mechanisms along the insulin signaling pathway improves beta-cell function under stress. *Diabetes* **59,** 2188–2197 CrossRef Medline
24. Torii, S., Saito, N., Kawano, A., Hou, N., Ueki, K., Kulkarni, R. N., and Takeuchi, T. (2009) Gene silencing of phogrin unveils its essential role in glucose-responsive pancreatic beta-cell growth. *Diabetes* **58,** 682–692 CrossRef Medline
25. Kubosaki, A., Gross, S., Miura, J., Saeki, K., Zhu, M., Nakamura, S., Hendriks, W., and Notkins, A. L. (2004) Targeted disruption of the IA-2β gene causes glucose intolerance and impairs insulin secretion but does not prevent the development of diabetes in NOD mice. *Diabetes* **53,** 1684–1691 CrossRef Medline
26. Cai, T., Hirai, H., Zhang, G., Zhang, M., Takahashi, N., Kasai, H., Satin, L. S., Leapman, R. D., and Notkins, A. L. (2011) Deletion of Ia-2 and/or Ia-2β in mice decreases insulin secretion by reducing the number of dense core vesicles. *Diabetologia* **54,** 2347–2357 CrossRef Medline
27. Mziaut, H., Kersting, S., Knoch, K. P., Fan, W. H., Trajkovski, M., Erdmann, K., Bergert, H., Ehehalt, F., Saeger, H. D., and Solimena, M. (2008) ICA512 signaling enhances pancreatic beta-cell proliferation by regulating cyclins D through STATs. *Proc. Natl. Acad. Sci. U.S.A.* **105,** 674–679 CrossRef Medline
28. Torii, S. (2009) Expression and function of IA-2 family proteins, unique neuroendocrine-specific protein-tyrosine phosphatases. *Endocr. J.* **56,** 639–648 CrossRef Medline
29. Saito, N., Takeuchi, T., Kawano, A., Hosaka, M., Hou, N., and Torii, S. (2011) Luminal interaction of phogrin with carboxypeptidase E for effective targeting to secretory granules. *Traffic* **12,** 499–506 CrossRef Medline
30. Torkko, J. M., Primo, M. E., Dirkx, R., Friedrich, A., Viehrig, A., Vergari, E., Borgonovo, B., Sönmez, A., Wegbrod, C., Lachnit, M., Münster, C., Sica, M. P., Ermácora, M. R., and Solimena, M. (2015) Stability of proICA512/IA-2 and its targeting to insulin secretory granules require β4-sheet-mediated dimerization of its ectodomain in the endoplasmic reticulum. *Mol. Cell. Biol.* **35,** 914–927 CrossRef Medline
31. Lingohr, M. K., Briaud, I., Dickson, L. M., McCuaig, J. F., Alárcon, C., Wicksteed, B. L., and Rhodes, C. J. (2006) Specific regulation of IRS-2 expression by glucose in rat primary pancreatic islet beta-cells. *J. Biol. Chem.* **281,** 15884–15892 CrossRef Medline
32. Rui, L., Fisher, T. L., Thomas, J., and White, M. F. (2001) Regulation of insulin/insulin-like growth factor-1 signaling by proteasome-mediated degradation of insulin receptor substrate-2. *J. Biol. Chem.* **276,** 40362–40367 CrossRef Medline
33. Ueyama, T., Kusakabe, T., Karasawa, S., Kawasaki, T., Shimizu, A., Son, J., Leto, T. L., Miyawaki, A., and Saito, N. (2008) Sequential binding of cytosolic Phox complex to phagosomes through regulated adaptor proteins: evaluation using the novel monomeric Kusabira-Green system and live imaging of phagocytosis. *J. Immunol.* **181,** 629–640 CrossRef Medline
34. Drake, P. G., Peters, G. H., Andersen, H. S., Hendriks, W., and Møller, N. P. (2003) A novel strategy for the development of selective active-site inhibitors of the protein tyrosine phosphatase-like proteins islet-cell antigen 512 (IA-2) and phogrin (IA-2β). *Biochem. J.* **373,** 393–401 CrossRef Medline
35. Woo, H. A., Yim, S. H., Shin, D. H., Kang, D., Yu, D. Y., and Rhee, S. G. (2010) Inactivation of peroxiredoxin I by phosphorylation allows localized H_2O_2 accumulation for cell signaling. *Cell* **140,** 517–528 CrossRef Medline
36. Muoio, D. M., and Newgard, C. B. (2008) Mechanisms of disease: molecular and metabolic mechanisms of insulin resistance and beta-cell failure in type 2 diabetes. *Nat. Rev. Mol. Cell Biol.* **9,** 193–205 CrossRef Medline
37. Kitamura, T., Nakae, J., Kitamura, Y., Kido, Y., Biggs, W. H., 3rd, Wright, C. V., White, M. F., Arden, K. C., and Accili, D. (2002) The forkhead transcription factor Foxo1 links insulin signaling to Pdx1 regulation of pancreatic beta cell growth. *J. Clin. Invest.* **110,** 1839–1847 CrossRef Medline
38. Porat, S., Weinberg-Corem, N., Tornovsky-Babaey, S., Schyr-Ben-Haroush, R., Hija, A., Stolovich-Rain, M., Dadon, D., Granot, Z., Ben-Hur, V., White, P., Girard, C. A., Karni, R., Kaestner, K. H., Ashcroft, F. M., Magnuson, M. A., *et al.* (2011) Control of pancreatic beta cell regeneration by glucose metabolism. *Cell Metab* **13,** 440–449 CrossRef Medline
39. Barr, A. J., Ugochukwu, E., Lee, W. H., King, O. N., Filippakopoulos, P., Alfano, I., Savitsky, P., Burgess-Brown, N. A., Müller, S., and Knapp, S. (2009) Large-scale structural analysis of the classical human protein tyrosine phosphatome. *Cell* **136,** 352–363 CrossRef Medline
40. Galic, S., Hauser, C., Kahn, B. B., Haj, F. G., Neel, B. G., Tonks, N. K., and Tiganis, T. (2005) Coordinated regulation of insulin signaling by the protein tyrosine phosphatases PTP1B and TCPTP. *Mol. Cell. Biol.* **25,** 819–829 CrossRef Medline
41. Togashi, Y., Shirakawa, J., Orime, K., Kaji, M., Sakamoto, E., Tajima, K., Inoue, H., Nakamura, A., Tochino, Y., Goshima, Y., Shimomura, I., and

Terauchi, Y. (2014) Beta-cell proliferation after a partial pancreatectomy is independent of IRS-2 in mice. *Endocrinology* **155,** 1643–1652 CrossRef Medline

42. Lin, X., Taguchi, A., Park, S., Kushner, J. A., Li, F., Li, Y., and White, M. F. (2004) Dysregulation of insulin receptor substrate 2 in beta cells and brain causes obesity and diabetes. *J. Clin. Invest.* **114,** 908–916 CrossRef Medline
43. Kubota, N., Terauchi, Y., Tobe, K., Yano, W., Suzuki, R., Ueki, K., Takamoto, I., Satoh, H., Maki, T., Kubota, T., Moroi, M., Okada-Iwabu, M., Ezaki, O., Nagai, R., Ueta, Y., *et al.* (2004) Insulin receptor substrate 2 plays a crucial role in beta cells and the hypothalamus. *J. Clin. Invest.* **114,** 917–927 CrossRef Medline
44. Terauchi, Y., Takamoto, I., Kubota, N., Matsui, J., Suzuki, R., Komeda, K., Hara, A., Toyoda, Y., Miwa, I., Aizawa, S., Tsutsumi, S., Tsubamoto, Y., Hashimoto, S., Eto, K., Nakamura, A., *et al.* (2007) Glucokinase and IRS-2 are required for compensatory beta cell hyperplasia in response to high-fat diet-induced insulin resistance. *J. Clin. Invest.* **117,** 246–257 CrossRef Medline
45. Gomi, H., Kubota-Murata, C., Yasui, T., Tsukise, A., and Torii, S. (2013) Immunohistochemical analysis of IA-2 family of protein tyrosine phosphatases in rat gastrointestinal endocrine cells. *J. Histochem. Cytochem.* **61,** 156–168 CrossRef Medline
46. Rother, K. I., Imai, Y., Caruso, M., Beguinot, F., Formisano, P., and Accili, D. (1998) Evidence that IRS-2 phosphorylation is required for insulin action in hepatocytes. *J. Biol. Chem.* **273,** 17491–17497 CrossRef Medline
47. Hou, N., Torii, S., Saito, N., Hosaka, M., and Takeuchi, T. (2008) Reactive oxygen species-mediated pancreatic beta-cell death is regulated by interactions between stress-activated protein kinases, p38 and c-Jun N-terminal kinase, and mitogen-activated protein kinase phosphatases. *Endocrinology* **149,** 1654–1665 CrossRef Medline
48. Hou, N., Mogami, H., Kubota-Murata, C., Sun, M., Takeuchi, T., and Torii, S. (2012) Preferential release of newly synthesized insulin assessed by a multi-label reporter system using pancreatic beta-cell line MIN6. *PLoS One* **7,** e47921 CrossRef Medline
49. Fukada, M., Kawachi, H., Fujikawa, A., and Noda, M. (2005) Yeast substrate-trapping system for isolating substrates of protein tyrosine phosphatases: isolation of substrates for protein tyrosine phosphatase receptor type z. *Methods* **35,** 54–63 CrossRef Medline
50. Kubota, C., Torii, S., Hou, N., Saito, N., Yoshimoto, Y., Imai, H., and Takeuchi, T. (2010) Constitutive reactive oxygen species generation from autophagosome/lysosome in neuronal oxidative toxicity. *J. Biol. Chem.* **285,** 667–674 CrossRef Medline